nature neuroscience

Perceptual decision making in less than 30 milliseconds

Terrence R Stanford, Swetha Shankar, Dino P Massoglia, M Gabriela Costello & Emilio Salinas

In perceptual discrimination tasks, a subject's response time is determined by both sensory and motor processes. Measuring the time consumed by the perceptual evaluation step alone is therefore complicated by factors such as motor preparation, task difficulty and speed-accuracy tradeoffs. Here we present a task design that minimizes these confounding factors and allows us to track a subject's perceptual performance with unprecedented temporal resolution. We find that monkeys can make accurate color discriminations in less than 30 ms. Furthermore, our simple task design provides a tool for elucidating how neuronal activity relates to sensory as opposed to motor processing, as demonstrated with neural data from cortical oculomotor neurons. In these cells, perceptual information acts by accelerating and decelerating the ongoing motor plans associated with correct and incorrect choices, as predicted by a race-to-threshold model, and the time course of these neural events parallels the time course of the subject's choice accuracy.

Perceptual decision-making capacity has been intensely studied in psychophysical and neurophysiological experiments as a function of signal quality, strength and subjective value[1–10]. However, there is a fundamental question that has been more difficult to address: how long does it take to make a perceptual judgment? This issue is relevant to many real-life situations in which a choice must be made very quickly. For example, a driver sees a traffic light and must rapidly decide whether to step on the brake or the accelerator. The ensuing action on the pedal will take at least a few hundred milliseconds to be initiated[11,12]. How much of this reaction time is dedicated to the perceptual analysis of the visual scene—that is, to determining whether the light is red or green?

The basic measurement seems deceptively simple. In well-trained macaque monkeys, which are the subjects of our study, a fixational eye movement (saccade) to a highly salient, unambiguous target takes ~150–200 ms to execute[13]. This must be the time that the motor apparatus needs to produce an unambiguous response, so the difference between this number and the reaction time in a two-alternative forced-choice task should be equal to the time that is necessary for making an additional sensory discrimination. Although this subtractive approach is a classic one[11,12,14–17], it has three shortcomings. First, forced-choice paradigms typically require cognitive resources other than just sensory analysis, such as working memory and a rule that links sensory stimuli to appropriate motor responses, so the two situations might not be directly comparable. Second, in tasks involving a sensory discrimination, the experimenter typically measures the point in time at which the motor action is initiated, but this is not necessarily the same as the point in time at which the sensory processing ends, which is what is needed. And third, when a change in a task parameter causes a change in reaction time, it is usually accompanied by a concurrent change in performance, and vice versa. Hence, a given change in reaction time might be caused either by an actual change in sensory processing speed or by an internal tradeoff between speed and accuracy to which the experimenter has no access.

Another approach is to manipulate the duration of stimulus presentation. Studies based on this idea[1,18–20] have shown that sensory information gradually accumulates over time to influence a behavioral choice, and that visual discrimination improves with stimulus duration. However, the accuracy with which sensory processing speed can be inferred by this method is limited, particularly for highly discriminable stimuli, which can be processed very rapidly. The main problem, besides the often necessary use of a mask[18,19] that introduces further complexities and unknown sources of variance[21,22], is again that changes in stimulus duration produce both variations in performance and large, correlated variations in reaction time (see the third point above).

The compelled-response paradigm described below largely avoids these problems and can be easily adapted to a variety of experimental conditions. Its crucial element is that the sensory cues to be discriminated (two colored spots in this experiment) are revealed after the go signal that instructs the subject to respond. Thus, the percentage of correct choices varies with the time gap between the go and the cues, whereas motor execution and mean reaction time remain approximately constant. This approach results in an accurate time course for perceptual performance, which can be temporally correlated with neuronal activity and from which sensory processing speed can be directly measured.

RESULTS

Task design

In the compelled-saccade task (**Fig. 1**), the subject first fixates on a central spot, and the color of this spot, red or green, indicates the color of the target. Then two yellow spots—potential targets—appear in the periphery. Next, the disappearance of the fixation spot is the go signal that tells the subject to initiate a saccade, although at this point the identities of the target and distracter are still unknown; these are

Department of Neurobiology and Anatomy, Wake Forest University School of Medicine, Winston-Salem, North Carolina, USA. Correspondence should be addressed to E.S. (esalinas@wfubmc.edu).

Received 3 September 2009; accepted 17 December 2009; published online 24 January 2010; doi:10.1038/nn.2485

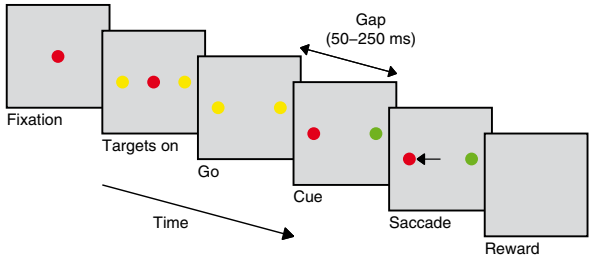

Figure 1 Sequence of events in the compelled-saccade task. A trial is correct if the subject makes an eye movement to the peripheral location that matches the color of the fixation spot (red in this example). The subject must initiate a response (left or right) when the fixation spot disappears (Go), although target and distracter are revealed after a gap of 50–250 ms (Cue).

revealed later, after a time gap that varies between 50 and 250 ms in duration, at the point marked 'cue'. At the cue, one yellow spot turns red and the other green. Finally, the monkey executes a saccade, and if the response is correct, a drop of liquid is given as a reward. The reaction time is the time between the onset of the go signal and the onset of the saccade, and the key parameter is the time gap, which varies pseudo-randomly across trials.

The idea behind the compelled-response paradigm is to separate the perceptual decision-making and motor-planning stages of the task by always instructing the subject when to respond. Because the motor response is triggered first, at the go signal, mean reaction times should stay approximately constant, and the perceptual information should influence a saccadic choice process that is already ongoing. The expected task performance is best understood at two extremes. At long or infinite gaps the sensory information never becomes available; the subject must guess which spot is the target because both of them are yellow. By contrast, at zero or short gaps the sensory information is revealed early; the subject can identify target and distracter and look at the appropriate spot (red or green). Thus, performance is expected to change systematically as a function of the gap but motor execution is not.

Motor and perceptual dependencies on the gap

We examined the behavior of two macaque monkeys trained to perform the compelled-saccade task. First we analyzed their eye movements (**Fig. 2**) and found that, for a given pair of targets, the velocity profiles generated in short- and long-gap trials were statistically identical. That is, for each monkey, the mean peak velocity was the same across gaps (Wilcoxon, $P > 0.25$ for both monkeys; **Fig. 2**), and so was the mean width at half-height (Wilcoxon, $P > 0.29$ for both monkeys; **Fig. 2**). Therefore, the gap had no discernible effect on saccadic execution.

By contrast, perceptual performance was strongly dependent on the gap, as revealed by the psychometric curves (**Fig. 3**). The percentage of correct choices was much higher at short gaps, when the cue was revealed early and subjects could discriminate the red and green spots, than at long gaps, when the cue was revealed late and subjects had to guess the target's location. Notably, however, mean reaction times changed little over this range of gaps (**Fig. 3b**), indicating that the monkeys did not try to wait for the cue (see **Supplementary Note 1** and **Supplementary Fig. 1**). So, as anticipated, variations in performance in the compelled-saccade task were largely dissociated from variations in motor execution.

The tachometric curve

Crucially, the behavioral data discussed above (**Fig. 3a**,**b**) can be sorted differently to directly reveal the perceptual processing speed of each subject. Before discussing that result, it is useful to consider a simple heuristic model that reproduces much of the observed behavior (**Fig. 4**). As in previous models[11,19,23–31], a saccadic choice is conceived as a race toward a threshold. In our case there are two variables, x_L and x_R, which represent the activities of two neuronal populations that trigger saccades to different locations. A movement to the left spot is produced if x_L reaches threshold first, whereas the movement is to the right when x_R wins the race. However, our model uniquely combines random and deterministic choices.

In each trial, the go signal starts the race (after an afferent delay); this means that a positive build-up rate is drawn for one of the variables and a lower or negative rate is drawn for the other. These initial rates are assigned randomly because at this point the two spots are still yellow. If x_L or x_R reaches threshold during this precue stage, the outcome of the race is a coin toss (**Fig. 4d**,**e**). However, once the cue information becomes available (after a total delay equal to gap plus afferent delay), the build-up rates change depending on the target and distracter locations. For instance,

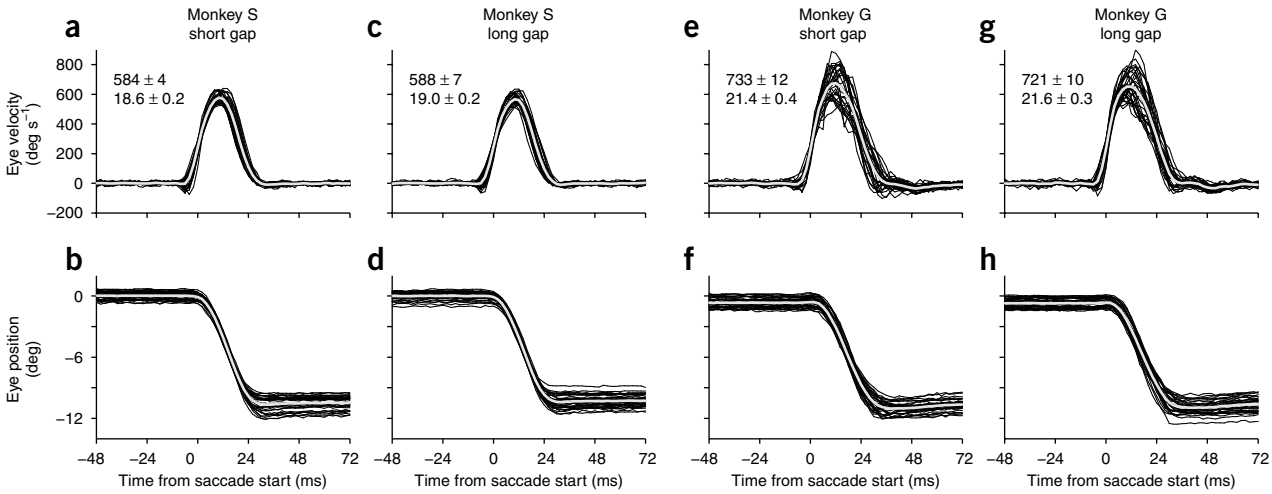

Figure 2 Oculomotor execution during the compelled-saccade task. (**a**,**b**) Eye velocity (**a**) and eye position (**b**) as functions of time for 30 saccades performed by monkey S in short-gap (50–100 ms) trials. Only horizontal components are shown. Black lines are single-trial traces; gray lines are averages. Numbers shown are mean peak velocity and mean width at half-height ± s.e.m. (**c**,**d**) Eye velocity (**c**) and eye position (**d**) as functions of time for 30 saccades performed by monkey S in long-gap (200–250 ms) trials. (**e**–**h**) As in **a**–**d**, except for 30 short-gap (**e**,**f**) and 30 long-gap (**g**,**h**) trials performed by monkey G.

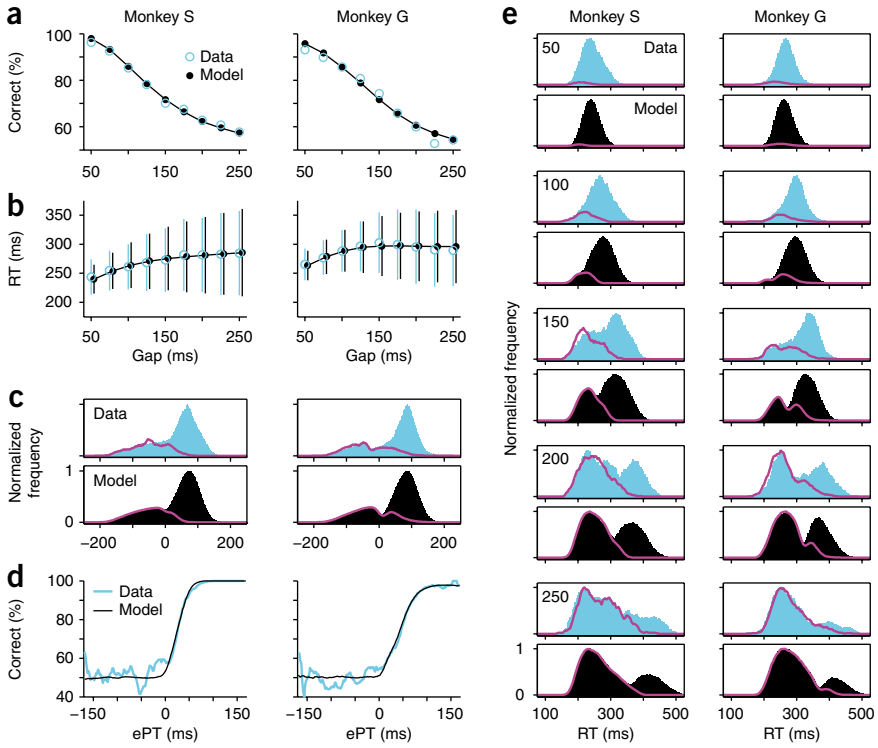

Figure 3 Behavioral and model performance in the compelled-saccade task. (**a**) Percentage of correct responses as a function of time gap (psychometric curve). Numbers of trials per point are $568 \le n \le 598$ for monkey S and $702 \le n \le 777$ for monkey G. (**b**) Mean reaction time (RT) ± 1 s.d. as a function of gap (chronometric curve). Each point includes both correct and incorrect trials. (**c**) Distributions of ePT values for correct (black and blue bars) and incorrect (magenta lines) trials. (**d**) Percentage of correct responses as a function of ePT (tachometric curve). (**e**) Distributions of reaction time values at five gaps. Gap values are indicated on upper left corners. RTs for correct (black and blue bars) and incorrect (magenta lines) trials are shown. In **c** and **d**, bin width is 20 ms; in **e** it is 40 ms. All results labeled 'Model' are from simulated trials generated with identical parameter values for each monkey.

consider a trial (**Fig. 4a**) in which initially x_L approached threshold faster than x_R, but then, because the target was on the right, x_L decelerated and x_R accelerated, with x_R eventually winning the race. One of the parameters in the model (τ in equation (3), Online Methods) is proportional to the speed with which the perceptual process occurs and therefore determines how fast x_L and x_R are accelerated (that is, how fast the cue information can alter the ongoing motor plans once the cue is revealed). In each trial, the model produces a reaction time and a motor outcome, left or right (for details, see Online Methods; see also **Supplementary Movie 1**).

Of particular importance, in this model the time during which the color information is available for guiding the choice in each trial, which we call the effective processing time (ePT), is clearly defined. It is

$$\text{ePT} = \text{RT} - \text{gap} - T_{ND} \qquad (1)$$

where the constant T_{ND} is the total non-decision time (afferent + efferent delay) and RT is reaction time. Note that this expression requires gap and reaction time values that are specific for each trial, not mean values. In the five examples in **Figure 4**, each ePT period is indicated by a horizontal bar. Races that end after the cue information becomes available have positive ePTs and an accuracy that increases with increasing ePT (**Fig. 4a–c**); by contrast, races that end before the cue information becomes available have negative ePTs and random outcomes (**Fig. 4d,e**), leading to 50% accuracy.

For each monkey, we fitted the model parameters to the experimental data (**Fig. 3a–d** and **Table 1**; see Online Methods). We computed an ePT for each trial performed by the monkeys by applying equation (1) using the T_{ND} value from the model. The resulting ePT distributions are shown in **Figure 3c**. Note that, for ePT ≤ 0, the ePT distributions for correct and incorrect trials are practically identical, indicating that, as in the model, performance is at chance in this range. By contrast, as ePT increases above 0 ms, a larger proportion of the trials tends to be correct.

The ePT is the amount of time during which the cue is effectively visible in each trial; it is the fundamental variable that determines perceptual performance in the compelled-saccade task. This is seen most clearly by plotting the percentage of correct responses as a

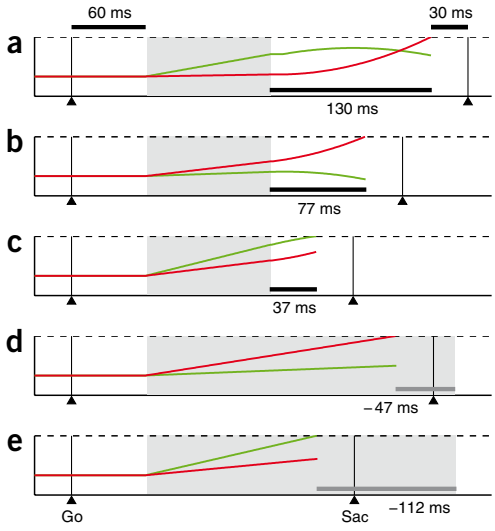

Figure 4 Five trials of the race-to-threshold model. Each plot shows the decision variables x_L (green) and x_R (red) as functions of time. Black triangles and vertical lines mark when the go signal is given (Go) and when the saccade is initiated (Sac); the interval between them is the reaction time. In these examples, x_L and x_R start racing 60 ms (afferent delay) after the go signal and a saccade is produced 30 ms (efferent delay) after threshold (dotted line) is crossed. Initially, build-up rates are drawn randomly and remain constant during the gap period (gray shade), but once the cue information becomes available (end of gray shade), the build-up rate for the target side (x_R in these examples) starts increasing and that for the distracter side starts decreasing. (**a–c**) Three trials with a 100-ms gap. (**d,e**) Two trials with a 250-ms gap. In all examples the target was red and was on the right, so **a**, **b** and **d** are correct and **c** and **e** are incorrect trials. Horizontal bars at the bottom indicate the ePT period in each trial; ePT values are positive (black) for races that are influenced by the sensory information (**a–c**) and negative (gray) for races that end before the cue information becomes available (**d,e**).

Table 1 Model parameter values in the standard compelled-saccade task and the motor bias experiment

Monkey/condition	r_G	σ_G	ρ	μ_I	σ_I	r_T	r_D	τ	T_{ND}	p_e
S/Standard CS	3.8	3.9	−0.6	7	2	36	−20	180	108	0
G/Standard CS	3.8	3	−0.8	20	10	340	−200	2,200	112	0.02
S/Motor bias, preferred side	7.5	4	−0.8	7	4	31	−12	90	109	0
S/Motor bias, non-preferred side	2.9	3.3	−0.8	7	4	17	−30	90	95	0

Times are in ms. CS, compelled-saccade task.

function of ePT. The resulting curve (**Fig. 3d**) can be referred to as a 'tachometric curve' because it reveals the speed of the perceptual process embedded in the task. For instance, for monkeys S and G, an accuracy of 75% was achieved with ePTs of 26 ± 2 ms (± s.e., from bootstrap) and 42 ± 2 ms, respectively. Of note, the parameter T_{ND} is not crucial to this analysis; it simply sets the origin of the *x*-axis in **Figure 3c**,**d** without affecting the shapes of the curves (see **Supplementary Note 2**). The key quantity is the difference between the reaction time and the gap in each trial, which we call the raw processing time (rPT).

Predicted and measured reaction time distributions

For each monkey, we found model parameter values that best fitted the data in **Figure 3a–d** (see Online Methods). Only the proportions of errors and the overall variability of the reaction times at each gap were used to fit the model. We then generated model reaction time distributions for correct and incorrect responses at each gap, with the idea that any salient features in the shapes of the simulated distributions would constitute specific predictions that we could analyze to validate the model.

Reaction time distributions obtained from the experiments and from computer simulations at various gaps are shown side by side in **Figure 3e**. The shapes of these distributions change markedly from short to long gaps, and the progression predicted by the model agrees well with that observed in the experimental data. The key is that the model mixes random choices (of 50% accuracy) with deterministic choices (of nearly 100% accuracy) in the right proportions for each gap. These correspond to the monkeys' guesses and informed discriminations, respectively. Further quantification of the match between model and experimental results is described in **Supplementary Note 3** and **Supplementary Figure 2**.

A motor bias experiment

We interpret the slope of the tachometric curve (**Fig. 3d**) as a direct indicator of the speed of the perceptual process that guides the subject's choices in the compelled-saccade task. If this is correct, then manipulations that alter the motor responses but not the perceptual difficulty of the task should lead to little or no change in slope. To test this, we varied the task conditions so that the monkeys would develop a motor bias: a tendency to make more saccades to one side than to the other[32]. We gave the monkeys a large reward (0.3 ml of juice) following correct saccades to one side and a small reward (0.1 ml) following correct saccades to the other (**Fig. 5**; see Online Methods). As a consequence, on average the animals chose the high-reward side about 76% of the time (75% for monkey S, 78% for monkey G; **Fig. 5a**). This result agrees well with the 3:1 ratio expected from Herrnstein's matching law[4,33,34] but does not capture the full complexity of the effects generated by the asymmetric reward, which depended strongly on the availability of the sensory information[32].

We analyzed the choices that the monkeys made to the high- and low-reward sides and found three prominent effects: first, the bias was stronger at long than at short gaps (**Fig. 5a**); second, responses in the high-reward direction were much more prone to errors than in the low-reward direction (**Fig. 5b**); and third, responses in the high-reward direction were also initiated sooner (**Fig. 5c**). Results are shown for monkey S only (**Fig. 5**) but were similar for monkey G (**Supplementary Note 4** and **Supplementary Fig. 3**). Crucially, in spite of these striking differences in motor execution, the slopes of the tachometric curves were not significantly different across reward conditions (monkey S, $P = 0.18$; monkey G, $P = 0.53$; permutation test). This, we believe, is because the perceptual discrimination itself did not change.

These results shed some light on how reward information and sensory evidence are combined when two motor responses are rewarded differently. They indicate that the low-reward side is chosen only if there is little uncertainty about the target's position (that is, when there is enough time to discriminate red from green accurately); otherwise, the high-reward side is the default. Two observations support this explanation. First, consider the ePT distributions

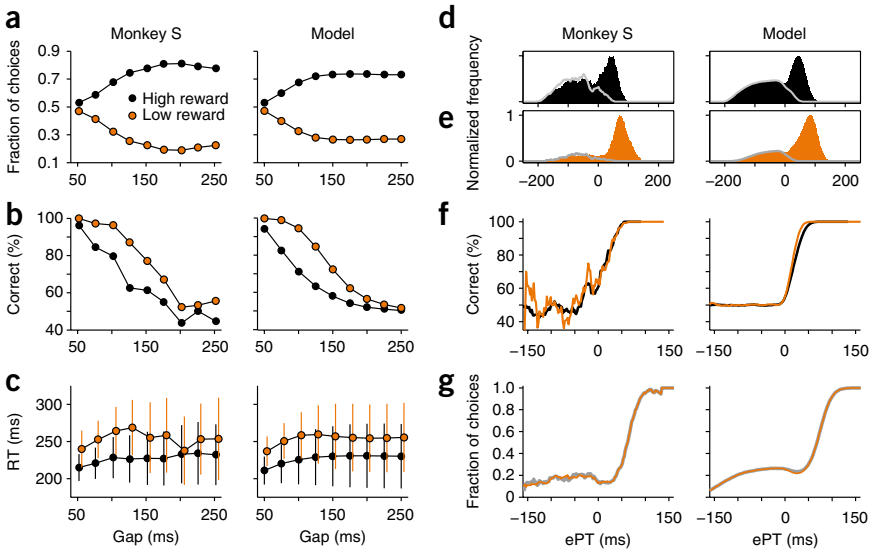

Figure 5 Behavioral and model performance in the motor-bias experiment. Trials are sorted according to choices, either toward the high-reward side (black) or the low-reward side (orange). (**a**) Fractions of saccades made to the high- and low-reward sides as functions of gap ($330 \le n \le 361$ trials per gap). (**b**) Percentages of correct choices as functions of gap. (**c**) Mean reaction times (RTs) ± 1 s.d. as functions of gap. (**d**) Distributions of ePT values for correct (black bars) and incorrect (gray lines) responses toward the high-reward side. (**e**) Distributions of ePT values for correct (orange bars) and incorrect responses (gray lines) toward the low-reward side. (**f**) Percentages of correct responses as functions of ePT for high- (black lines) and low- (orange lines) reward trials. (**g**) For each ePT, the curves show the fraction of all saccades (orange lines) or of all correct saccades (gray lines) made to the low-reward side. ePT bin size is 20 ms.

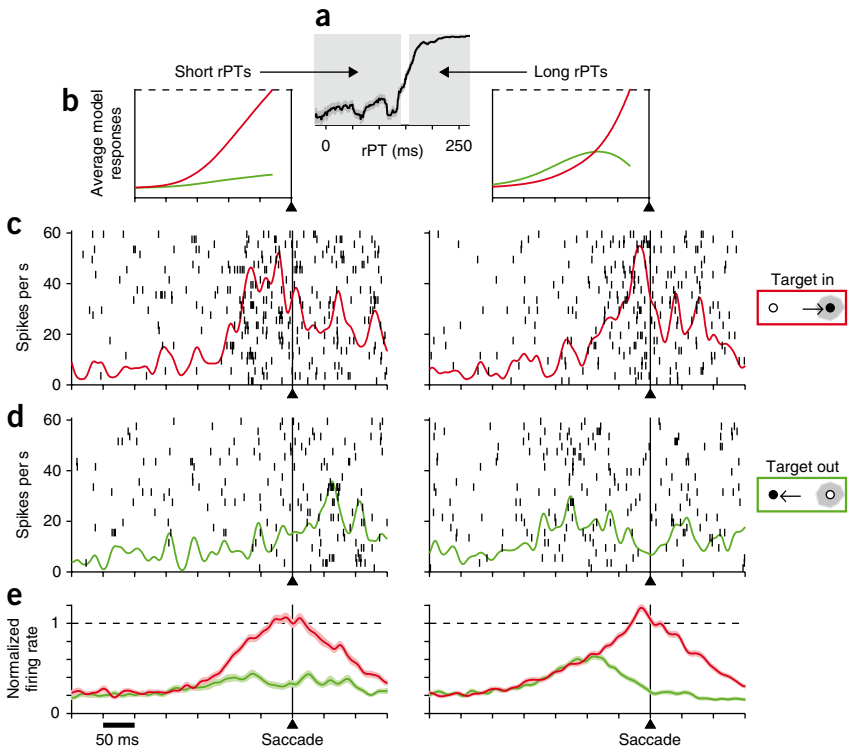

Figure 6 Oculomotor activity during the compelled-saccade task. (**a**) Tachometric curve obtained from all recording sessions; $n = 7{,}282$ trials. The x axis is rPT (rPT = reaction time – gap). Shaded areas indicate short- and long-rPT groups. (**b**) Mean time courses of the decision variables x_L and x_R synchronized on threshold crossing (dashed line), with saccades assumed to occur 30 ms later (triangles and vertical lines). Correct model responses into (red) and away from (green) the movement field are shown for short (left side) and long (right side) rPTs. (**c**) Responses of a single FEF neuron during correct trials into the movement field, for short (left side) and long (right side) rPTs. Each panel shows spike trains from 30 trials synchronized on saccade onset (triangles and vertical lines). Firing rates as functions of time (red traces) were obtained by convolving the spikes with a Gaussian of $\sigma = 6$ ms. The key on the right indicates the positions of the movement field (gray patch), target (filled circle) and distracter (open circle). (**d**) Responses from the same cell as in **c** but for correct saccades away from the movement field. (**e**) Average firing rates of 30 FEF neurons as functions of time. For each cell, activity was normalized by the firing rate at saccade onset in short-rPT trials into the movement field. Light colors indicate ± 1 s.e.m. Note differences between short- (left side) and long-rPT (right side) responses.

obtained for correct and error trials. For high-reward choices the results are consistent with a large fraction of guesses (**Fig. 5d**), whereas for low-reward choices the results are consistent with most perceptual judgments being correct (**Fig. 5e**). Second, consider the fraction of choices made to the low-reward side as a function of ePT (**Fig. 5g**). The curve shows that the monkey's preference varied sharply as a function of ePT (compare to the weak dependence as a function of gap shown in **Fig. 5a**). Therefore, the amount of time during which a monkey is exposed to the sensory cue—that is, the ePT—is an excellent predictor of its choice. This effect was also seen in the model (**Fig. 5g**), which, with minor modifications (see Online Methods), could reproduce quite accurately the main differences between high- and low-reward choices (**Fig. 5**, 'Model').

Neuronal sensitivity to processing time

In our race model, x_L and x_R are conceived as the firing rates of two populations of neurons that generate movements to the left and right targets but are also influenced by perceptual information[8,19,28,35–39]. If this representation is correct, oculomotor neurons in cortical areas that participate in the saccadic choice process should qualitatively behave like x_L and x_R; in particular, they should exhibit similar dependencies on processing time. To investigate this, we recorded neuronal activity from oculomotor neurons in the frontal eye field (FEF) while monkeys S and G performed the compelled-saccade task. We report results from a population of 30 neurons, 18 from monkey S and 12 from monkey G, that had stereotypical motor properties[24,40] and little or no sensory-evoked activity (see Online Methods, **Supplementary Note 5** and **Supplementary Fig. 4**). Such 'movement' cells were selected because they correspond most closely to the model variables x_L and x_R.

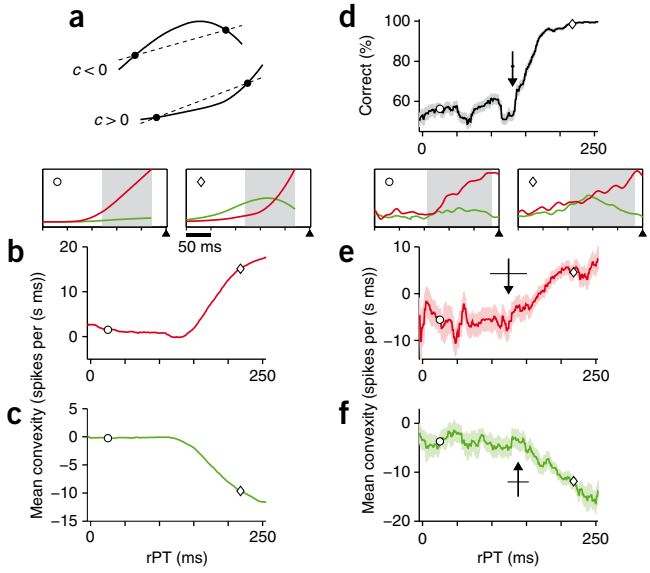

Figure 7 Sensory information accelerates oculomotor activity. (**a**) The mean convexity c between two points on a curve is computed as the average difference between the line that joins those points (dotted line) and the curve values (continuous traces). (**b**,**c**) Mean convexity of the trajectories of the model variables x_L and x_R as a function of rPT. Red and green lines indicate correct trials into and away from the movement field, respectively. Insets above **b** show mean trajectories obtained in two rPT bins (keyed by a circle and a diamond). Shaded areas indicate the interval used to calculate convexity. (**d**) Tachometric curve from all recording sessions. Arrow indicates the transition point at which the curve starts increasing. Horizontal line across arrow indicates error s.d. (from jackknife; see Online Methods). (**e**,**f**) Mean convexity of the FEF population activity as a function of rPT, for correct trials into (red) and away from (green) the movement field. Light colors indicate ± 1 s.e.m. Arrows indicate transition points and horizontal lines are error s.d. (from jackknife). Before averaging across cells, rates were normalized as in **Figure 6e**. Other conventions as in **b**,**c**. rPT bin size is 40 ms.

In a first analysis, we subdivided all recorded trials into short- and long-rPT groups (**Fig. 6a**) and compared the neuronal responses across groups. Recall that in short-rPT trials choices are not guided by sensory information, whereas in long-rPT trials they are. According to the model, the fundamental action of the cue information is to accelerate the developing motor plan for the target side and decelerate the plan for the distracter side, producing curved trajectories (**Fig. 4a–c**). Here we mean acceleration in the literal, physical sense because the cue information changes the second derivatives of the decision variables x_L and x_R (equation (3)). By averaging over many simulated trials, this effect becomes manifest in two ways: first, the oculomotor activity leading to saccades away from the cells' movement field should be stronger with long rPTs than with short rPTs but should also decline markedly before movement onset (**Fig. 6b**, green traces); and second, the activity leading to saccades into the movement field should rise to threshold more steeply with long than with short rPTs (**Fig. 6b**, red traces). Are these patterns found in the neural data?

The responses of a single neuron during the compelled-saccade task are shown in **Figure 6c,d**. Activity is aligned on saccade onset, with trials sorted according to saccade direction (**Fig. 6c**, into the movement field; **Fig. 6d**, away from the movement field) and processing time (left side, short rPTs; right side, long rPTs). This unit's behavior was generally consistent with the model, but its responses were variable, as expected. However, the population average agreed well with the model's predictions: before saccades away from the movement field (**Fig. 6e**, green traces), the firing rate reaches a higher level and then declines more sharply at long rPTs than at short rPTs (see ref. 31); and before saccades into the movement field (**Fig. 6e**, red traces), the firing rate trajectory is steeper at long rPTs than at short ones. This difference in curvature is subtle but was highly significant ($P = 0.0006$, permutation test).

Temporal correlates of choice accuracy

In the compelled-saccade task, performance changes sharply with the amount of exposure to the sensory cue. We hypothesized that, as a function of rPT, the neural activity associated with the oculomotor choice should change with a time course similar to that observed behaviorally. To test this, we measured the mean convexity of the firing rate trajectories as a function of rPT. We chose convexity because this quantity is closely related to acceleration and its calculation is simple and robust to noise (**Fig. 7a**). Trajectories that decelerate have negative convexity and curve downward, whereas trajectories that accelerate have positive convexity and curve upward.

We first analyzed the convexity associated with the model variables x_L and x_R and found that the responses in and out of the movement field behave in opposite ways as functions of rPT: the former have an approximately constant convexity at first, which then increases steadily (**Fig. 7b**), whereas for the latter, the convexity also stays constant initially but then decreases toward strongly negative values (**Fig. 7c**). This simply restates the result in **Fig. 6b** and quantifies it with a fine temporal grain. That is, the firing rate trajectories should curve upward before correct saccades into the movement field, whereas they should turn downward before correct saccades away from the movement field. Crucially, however, both effects must start at about the same time as the subject's rise in performance (**Fig. 7d**), and their magnitude must depend on the amount of exposure to the cue.

This prediction was verified. We plotted the mean convexity of the neuronal responses as a function of rPT for trials into (**Fig. 7e**) and away from (**Fig. 7f**) the movement field. The results from the 30 FEF neurons were noisy, but the time courses clearly matched those expected from the model. In particular, the two transition points at which convexity starts changing steadily (arrows in **Fig. 7e,f**) occurred very close to each other and to the transition point of the tachometric curve, as predicted (transition points were determined by fitting the data with analytical functions that contain such transitions; see Online Methods). Furthermore, after the transitions, the slopes of the convexity plots were highly significant ($P = 0.002$ and $P = 0.0004$ for trials into and away from the movement field, respectively; permutation test). Therefore, during the task the cue information accelerates the motor plan for the target and decelerates the plan for the distracter—the main premise of the race model—and the onset of these dynamic changes coincides with the onset of the subject's rise in performance above chance.

DISCUSSION

The compelled-response paradigm presented here can, to a large extent, decouple the perceptual-evaluation and motor-execution steps of a behavioral choice. Part of its success depends on simultaneously controlling the timing of the sensory information (cue) and the response trigger (go), as suggested by earlier studies in motor control[41,42], but its minimalistic design goes much further: it achieves fine temporal resolution in a perceptual discrimination process without additional stimuli or masks, and monkeys readily learn the task. The resulting tachometric curve is an excellent diagnostic of perceptual ability because performance varies much more rapidly with ePT (**Fig. 3d**) than with reaction time or with gap (**Fig. 3a**). This means that, by computing the tachometric curve, an important source of variability unrelated to sensory processing is filtered out. However, this calculation is achieved very simply (equation (1)).

Our results indicate that, given highly discriminable stimuli, color information needs to be processed for just 25–50 ms to have a sizeable impact on behavioral outcome. But note that our model does not attribute this processing time to a specific color-sensitive area, such as the retina, or area V4, and that it also remains agnostic regarding the biophysical origin of this time scale (that is, whether it results from slow sensory transduction or from internal noise in more central circuits[25,26,36,38], for instance). What the model does show is that such a time scale for sensory processing is consistent with all the behavioral data in the task—reaction time distributions, choice preferences under bias, and so on—and with the oculomotor activity observed in the FEF.

Our results provide converging evidence that, within a choice process that takes a few hundred milliseconds, the sensory evaluation step might consume much less than 100 ms, as suggested by previous experiments[43–46]. In particular, our findings are close to the measurement of ~25 ms made in humans[46], and which probably reflects the minimum time necessary for color identification only, without the computational overhead needed to compare two stimuli and communicate the result of the discrimination (red or green) to the correct motor output (left or right) on the fly. Our results are also in agreement with an earlier study of FEF visuomotor cells[43], which showed that an ideal observer can reliably differentiate the activity evoked by a target from that evoked by a distracter within ~25 ms of the onset of neural discrimination, on average. However, the key advantage of the present approach is that it does not require any assumptions about the relationship between neuronal and behavioral performance (for example, identities and numbers of participating neurons, ideal-observer criterion) but rather is based on a direct behavioral manifestation of the subject's perceptual discrimination process—the tachometric curve—which explicitly depicts how the perceptual decision unfolds in time.

More generally, the techniques described here can be used to understand how reward contingencies and perceptual knowledge are combined, as shown with the motor bias experiment, and to reveal how perceptual and motor processes interact, as illustrated with the FEF data. Furthermore, the present task design is not limited to color discrimination; it can be extended to investigate processing speed under many other experimental conditions. For instance, the task can be easily adapted to the auditory modality and to visual features other than color, such as object shape or motion direction. These applications will be explored in future studies.

METHODS

Methods and any associated references are available in the online version of the paper at http://www.nature.com/natureneuroscience/.

Note: Supplementary information is available on the Nature Neuroscience website.

ACKNOWLEDGMENTS

Research was supported by the National Institutes of Health/National Eye Institute grant R01 EY12389 to T.R.S.

AUTHOR CONTRIBUTIONS

T.R.S. conceived the task, supervised all experiments and data analyses, and co-wrote the manuscript; S.S. contributed to the collection, analysis and modeling of the behavioral data; D.P.M. contributed to the design of the experiments and to the collection of behavioral data; M.G.C. contributed to the collection of behavioral data and to the collection and analysis of neural data; E.S. developed the race model, contributed to the experimental design and data analysis and co-wrote the manuscript.

COMPETING INTERESTS STATEMENT

The authors declare no competing financial interests.

Published online at http://www.nature.com/natureneuroscience/.
Reprints and permissions information is available online at http://npg.nature.com/reprintsandpermissions/.

1. Britten, K.H., Shadlen, M.N., Newsome, W.T. & Movshon, J.A. The analysis of visual motion: a comparison of neuronal and psychophysial performance. *J. Neurosci.* **12**, 4745–4765 (1992).
2. Dodd, J.V., Krug, K., Cumming, B.G. & Parker, A.J. Perceptually bistable three-dimensional figures evoke high choice probabilities in cortical area MT. *J. Neurosci.* **21**, 4809–4821 (2001).
3. Ernst, M.O. & Banks, M.S. Humans integrate visual and haptic information in a statistically optimal fashion. *Nature* **415**, 429–433 (2002).
4. Sugrue, L.P., Corrado, G.S. & Newsome, W.T. Matching behavior and the representation of value in the parietal cortex. *Science* **304**, 1782–1787 (2004).
5. de Lafuente, V. & Romo, R. Neuronal correlates of subjective sensory experience. *Nat. Neurosci.* **8**, 1698–1703 (2005).
6. McCoy, A.N. & Platt, M.L. Risk-sensitive neurons in macaque posterior cingulate cortex. *Nat. Neurosci.* **8**, 1220–1227 (2005).
7. Nieder, A. & Merten, K. A labeled-line code for small and large numerosities in the monkey prefrontal cortex. *J. Neurosci.* **27**, 5986–5993 (2007).
8. Churchland, A.K., Kiani, R. & Shadlen, M.N. Decision-making with multiple alternatives. *Nat. Neurosci.* **11**, 693–702 (2008).
9. Gu, Y., Angelaki, D.E. & DeAngelis, G.C. Neural correlates of multisensory cue integration in macaque MSTd. *Nat. Neurosci.* **11**, 1201–1210 (2008).
10. Matsumora, T., Koida, K. & Komatsu, H. Relationship between color discrimination and neural responses in the inferior temporal cortex of the monkey. *J. Neurophysiol.* **100**, 3361–3374 (2008).
11. Luce, R.D. *Response Times: Their Role in Inferring Elementary Mental Organization* (Oxford Univ. Press, Oxford, UK, 1986).
12. Sanders, A.F. *Elements of Human Performance: Reaction Processes and Attention in Human Skill* (Erlbaum, Mahwah, New Jersey, USA, 1998).
13. Paré, M. & Munoz, D.P. Saccadic reaction time in the monkey, advanced preparation of oculomotor programs is primarily responsible for express saccade occurrence. *J. Neurophysiol.* **76**, 3666–3681 (1996).
14. Donders, F.C. 1868. On the speed of mental processes. Translated by W. G. Koster. *Acta Psychol. (Amst.)* **30**, 412–431 (1969).
15. Sternberg, S. High speed scanning in human memory. *Science* **153**, 652–654 (1966).
16. Posner, M.I. *Chronometric Explorations of Mind* (Erlbaum, Hillsdale, New Jersey, USA, 1978).
17. Meyer, D.E., Osman, A.M., Irwin, D.E. & Yantis, S. Modern mental chronometry. *Biol. Psychol.* **26**, 3–67 (1988).
18. Bergen, J.R. & Julesz, B. Parallel versus serial processing in rapid pattern discrimination. *Nature* **303**, 696–698 (1983).
19. Ratcliff, R. & Rouder, J.N. A diffusion model account of masking in two-choice letter identification. *J. Exp. Psychol. Hum. Percept. Perform.* **26**, 127–140 (2000).
20. Kiani, R., Hanks, T.D. & Shadlen, M.N. Bounded integration in parietal cortex underlies decisions even when viewing duration is dictated by the environment. *J. Neurosci.* **28**, 3017–3029 (2008).
21. Breitmeyer, B.G. & Ogmen, H. Recent models and findings in visual backward masking: a comparison, review, and update. *Percept. Psychophys.* **62**, 1572–1595 (2000).
22. Breitmeyer, B.G., Ro, T. & Ogmen, H. A comparison of masking by visual and transcranial magnetic stimulation: implications for the study of conscious and unconscious visual processing. *Conscious. Cogn.* **13**, 829–843 (2004).
23. Carpenter, R.H.S. & Williams, M.L.L. Neural computation of log likelihood in control of saccadic eye movements. *Nature* **377**, 59–62 (1995).
24. Hanes, D.P. & Schall, J.D. Neural control of voluntary movement initiation. *Science* **274**, 427–430 (1996).
25. Smith, P.L. & Ratcliff, R. Psychology and neurobiology of simple decisions. *Trends Neurosci.* **27**, 161–168 (2004).
26. Palmer, J., Huk, A.C. & Shadlen, M.N. The effect of stimulus strength on the speed and accuracy of a perceptual decision. *J. Vis.* **5**, 376–404 (2005).
27. Lo, C.C. & Wang, X.J. Cortico-basal ganglia circuit mechanism for a decision threshold in reaction time tasks. *Nat. Neurosci.* **9**, 956–963 (2006).
28. Wong, K.F. & Wang, X.J. A recurrent network mechanism of time integration in perceptual decisions. *J. Neurosci.* **26**, 1314–1328 (2006).
29. Boucher, L., Palmeri, T.J., Logan, G.D. & Schall, J.D. Inhibitory control in mind and brain: an interactive race model of countermanding saccades. *Psychol. Rev.* **114**, 376–397 (2007).
30. Brown, S.D. & Heathcote, A. The simplest complete model of choice response time: linear ballistic accumulation. *Cogn. Psychol.* **57**, 153–178 (2007).
31. Ratcliff, R., Hasegawa, Y.T., Hasegawa, R.P., Smith, P.L. & Segraves, M.A. Dual diffusion model for single-cell recording data from the superior colliculus in a brightness-discrimination task. *J. Neurophysiol.* **97**, 1756–1774 (2007).
32. Feng, S., Holmes, P., Rorie, A. & Newsome, W.T. Can monkeys choose optimally when faced with noisy stimuli and unequal rewards? *PLoS Comput. Biol.* **5**, e1000284 (2009).
33. Herrnstein, R.J. Relative and absolute strength of responses as a function of frequency of reinforcement. *J. Exp. Anal. Behav.* **4**, 267–272 (1961).
34. Soltani, A. & Wang, X.J. A biophysically based neural model of matching law behavior: melioration by stochastic synapses. *J. Neurosci.* **26**, 3731–3744 (2006).
35. Horwitz, G.D. & Newsome, W.T. Separate signals for target selection and movement specification in the superior colliculus. *Science* **284**, 1158–1161 (1999).
36. Wang, X.J. Probabilistic decision making by slow reverberation in cortical circuits. *Neuron* **36**, 955–968 (2002).
37. Schall, J.D. Neural correlates of decision processes: neural and mental chronometry. *Curr. Opin. Neurobiol.* **13**, 182–186 (2003).
38. Beck, J.M. *et al.* Probabilistic population codes for Bayesian decision making. *Neuron* **60**, 1142–1152 (2008).
39. Salinas, E. So many choices: what computational models reveal about decision-making mechanisms. *Neuron* **60**, 946–949 (2008).
40. Bruce, C.J. & Goldberg, M.E. Primate frontal eye fields. I. Single neurons discharging before saccades. *J. Neurophysiol.* **53**, 603–635 (1985).
41. Hening, W., Favilla, M. & Ghez, C. Trajectory control in targeted force impulses. V. Gradual specification of response amplitude. *Exp. Brain Res.* **71**, 116–128 (1988).
42. Ghez, C., Hening, W. & Favilla, M. Gradual specification of response amplitude in human tracking performance. *Brain Behav. Evol.* **33**, 69–74 (1989).
43. Thompson, K.G., Hanes, D.P., Bichot, N.P. & Schall, J.D. Perceptual and motor processing stages identified in the activity of macaque frontal eye field neurons during visual search. *J. Neurophysiol.* **76**, 4040–4055 (1996).
44. Ludwig, C.J., Gilchrist, I.D., McSorley, E. & Baddeley, R.J. The temporal impulse response underlying saccadic decisions. *J. Neurosci.* **25**, 9907–9912 (2005).
45. Ghose, G.M. Strategies optimize the detection of motion transients. *J. Vis.* **6**, 429–440 (2006).
46. Bodelón, C., Fallah, M. & Reynolds, J.H. Temporal resolution for the perception of features and conjunctions. *J. Neurosci.* **27**, 725–730 (2007).

ONLINE METHODS

Behavior and electrophysiology. All protocols complied with NIH guidelines, USDA regulations and policies set forth by the Institutional Animal Care and Use Committee of Wake Forest University School of Medicine. Before training, under general anesthesia, an MRI-compatible titanium post was attached to each monkey's skull. The post served to stabilize their heads during subsequent experimental sessions. In monkey S, eye movements were monitored with an eye coil that provided an analog eye-position signal at a rate of 500 Hz. For monkey G, we used an EyeLink1000 infrared tracking system (SR Research) with a sampling rate of 1,000 Hz. Color stimuli were delivered through an array of light-emitting diodes placed at a viewing distance of 145 cm from the monkey's chair. Pairs of saccade targets were separated by 10–20° of visual angle. Reaction time was measured as the amount of time from the go signal until the velocity of the saccade reached a cutoff value of 50° s^{-1}. To discourage the monkeys from waiting for the cue, they were allowed to initiate a response up to 600 ms after the go signal, and a trial was aborted if the response took longer. In the motor bias sessions, large and small rewards were 0.3 and 0.1 ml in volume, respectively. The high-reward side was kept constant for a block of 150–250 trials and was then switched. In all conditions, standard and biased, red and green targets were presented with equal probability at all target locations.

In both monkeys, stereotactic coordinates and MRI images were used to place a recording cylinder (20 mm diameter) over the arcuate sulcus of the frontal cortex. Putative FEF neurons were recorded using tungsten microelectrodes (FHC). The majority of neurons reported on here (23/30) were constrained to recording sites in which we verified that saccade-like eye movements could be evoked with microstimulation at low current threshold (<50 μA). Once a single unit was isolated, a single-target delayed-saccade task was used to render an online estimate of preferred response direction and eccentricity before testing with the compelled-saccade task. To explore the predictions of the present model, we explicitly chose for analysis a subset of neurons having strong saccade-related bursts but little or no transient activation linked to stimulus onset (see **Supplementary Note 5** and **Supplementary Fig. 4**).

Modeling. The race-to-threshold model has ten free parameters that varied for each monkey. The free parameters were optimized to minimize the root-mean-square error between the simulated and the experimental data for each animal. In the standard compelled-saccade task, the error function had six terms, one for each of the curves in **Figure 3a–d** plus one for the s.d. included in **Figure 3b**. All simulations were run in Matlab (The Mathworks). **Supplementary Movie 1** shows ten simulated trials. A Matlab script that replicates the model results in **Figure 3** is available from the authors upon request.

In the race model, the competing variables x_R and x_L represent developing motor plans (**Supplementary Note 6**). They start at 0 and the race is over when one of them reaches a threshold of 1,000 (arbitrary units). When x_L (x_R) wins, the oculomotor response is considered to be to the left (right). In each simulated trial there are two integration stages, a random and a deterministic one. In the first stage of each race, before the cue information is available, the two build-up rates, r_R and r_L, are drawn from a bivariate Gaussian distribution with mean r_G (same for both variables), s.d. σ_G (same for both variables) and correlation coefficient ρ. Thus, x_R and x_L change according to

$$\begin{aligned} dx_R/dt &= r_R \\ dx_L/dt &= r_L \end{aligned} \qquad (2)$$

where the rates are constant. Because ρ is negative, one variable tends to approach threshold faster than the other, but this assignment is random in each trial. This integration process lasts a time equal to the gap plus ΔT, where ΔT is drawn from a Gaussian distribution with zero mean and s.d. of 10 ms. The term ΔT represents variability in the afferent delay (or whatever processes occur before the integration starts). The second stage of the race begins gap + ΔT ms after the start of the first stage, at which point the target and distracter locations become known to the circuit. At this transition, two things happen. First, the integration is halted for a time T_I, which is drawn from a Gaussian distribution with mean μ_I and s.d. σ_I, but such that any negative T_I values are discarded. This interruption time is not essential to the model but accounts for a small dip near zero that is often seen in the ePT distributions (most obvious in **Fig. 3c**, Monkey G). During T_I, none of the variables change. Second, integration is resumed after the interruption, but the build-up rates start changing toward asymptotic values r_T for target (large, positive value) and r_D for distracter (negative value). For instance, if the target is on the right, the rate for x_R begins to change toward r_T and the rate for x_L begins to change toward r_D. That is, during this second stage, x_L and x_R still follow the equations above, but also

$$\begin{aligned} dr_R/dt &= (r_T - r^0{}_R)/\tau \\ dr_L/dt &= (r_D - r^0{}_L)/\tau \end{aligned} \qquad (3)$$

where $r^0{}_R$ and $r^0{}_L$ are the rate values drawn originally, during the first stage, and τ is the time required to reach the final values r_T and r_D. We stress that these equations (equation (3)) apply only after the cue has been revealed. Once r_R and r_L are equal to r_T and r_D, respectively, they do not change any more. Of course, if the target is on the left, then r_L tends to r_T and r_R tends to r_D instead. The integration process (equation (2)) continues until x_L or x_R reaches threshold. In most trials, the build-up rates r_R and r_L are correctly assigned according to the target and distracter locations, as described. However, there is a small probability p_e that this assignment is incorrect (reversed). This accounts for trials in which, even though the ePT is long, the response is wrong (for example, the curve for monkey G in **Fig. 3d** does not reach 100%). The duration of the second stage is equal to the ePT. The reaction time in each trial is computed as RT = gap + ePT + T_{ND}, where T_{ND} is the total non-decision time. Note that although it is easier to think of separate afferent and efferent delays (as in **Fig. 4**) the model is sensitive only to the total non-decision time T_{ND} (see **Supplementary Note 2**). Parameter values are listed in **Table 1**.

In simulations of the motor-bias experiment, the race model is the same but the parameters that determine x_R and x_L are no longer identical (the only exception is τ). For instance, in the first stage of each race, the two build-up rates, r_R and r_L, are now drawn from a bivariate Gaussian distribution with means $r_G + \Delta r_G$ (for r_R) and $r_G - \Delta r_G$ (for r_L), s.d. $\sigma_G + \Delta\sigma_G$ (for r_R) and $\sigma_G - \Delta\sigma_G$ (for r_L), and correlation coefficient ρ. The bias terms Δr_G and $\Delta\sigma_G$ thus make the left and right sides asymmetric. With such manipulation, the model still generates random choices before the cue information is revealed, but it tilts the odds in favor of one side (**Table 1**).

Statistical analysis. We obtained several curves with a particular characteristic in common: they remain approximately flat for a certain range of x-axis values and then start increasing or decreasing steadily (**Fig. 7b–f**). We refer to the point at which the slope becomes nonzero in those curves as the transition point x_{trans}. This is an important quantity in our analysis, because according to the model (**Fig. 7b,c**), it should be nearly the same for the tachometric curve (**Fig. 7d**) and for the two convexity curves derived from the neuronal data (**Fig. 7e,f**). We estimated x_{trans} as follows. For a given curve, we fitted the data to an analytic function composed of two line segments, a flat segment and a non-flat segment, that intersect at x_{trans}. We refer to this as a threshold-linear function. Each threshold-linear function is characterized by three parameters: the height of the flat segment along the y-axis, the slope of the non-flat segment and the transition point x_{trans}. Optimal parameter values were found with standard algebraic methods used to fit a single straight line to a dataset (least-squares minimization). For details, see **Supplementary Note 7** and **Supplementary Figure 5**.

The error in x_{trans} was estimated using the jackknife method, which is based on the idea of recalculating a statistic multiple times, each time deleting a different contributing sample[47,48]. In our case, we recalculated x_{trans} 30 times, on each pass omitting the data contributed by one of the recorded neurons and repeating the fit.

Finally, each linear-threshold fit produced a slope for the increasing or decreasing part of a curve. To calculate its significance we used a permutation test[49]. For each curve, we shuffled the values on the y-axis and computed the slope of the line that best fitted the shuffled data between x_{trans} and the maximum rPT value used in the original fit. This randomization was repeated 5,000 times. Then we computed the fraction of times that the slopes of the randomized data equaled or exceeded the slope of the original, non-shuffled data. This fraction was taken as the probability of having observed the original slope value by chance, when there was actually no correlation between the quantities on the x and y axes.

47. Efron, B. *The Jackknife, the Bootstrap and Other Resampling Plans* (Society for Industrial and Applied Mathematics, Philadelphia, 1982).
48. Davison, A.C. & Hinkley, D. *Bootstrap Methods and Their Applications* (Cambridge Univ. Press, Cambridge, UK, 2006).
49. Siegel, S. & Castellan, N.J. *Nonparametric Statistics for the Behavioral Sciences* (McGraw-Hill, Boston, 1988).

doi:10.1038/nn.2485